International Journal of Applied Power Engineering (IJAPE)
Vol. 15, No. 1, March 2026, pp. 69∼79
ISSN: 2252-8792, DOI: 10.11591/ijape.v15.i1.pp69-79

Enhancing electrolyzer performance for hydrogen production in a solar system using a buck converter with sliding mode control

Abdellah El Idrissi[1], Belkasem Imodane[1], M'hand Oubella[1], Hatim Ameziane[2], Mohamed Benydir[1], Kaoutar Dahmane[1], Driss Belkhiri[1], Mohamed Ajaamoum[1]
[1]Laboratory of Engineering Sciences and Energy Management (LASIME), National School of Applied Sciences, Ibn Zohr University, Agadir, Morocco
[2]Laboratory of Science and Technology for the Engineer (LaSTI), Electrical Engineering Department, National School of Applied Sciences (ENSA), Sultan Moulay Slimane University, Khouribga, Morocco

Article Info

Article history:

Received Jan 12, 2025
Revised Aug 26, 2025
Accepted Oct 16, 2025

Keywords:

DC-DC converter
Electrolyzer
Hydrogen production
Renewable energy
Sliding mode control

ABSTRACT

As the world increasingly turns to renewable energy, green hydrogen produced through water electrolysis has emerged as a clean and promising alternative to fossil fuels. In this work, we explore a solar-powered hydrogen production system that uses real data from an operational photovoltaic (PV) installation, ensuring accurate and realistic modeling of environmental conditions. A DC-DC buck converter is used to regulate the fluctuating PV output, supplying the precise voltage needed by a PEM electrolyzer. Sliding mode control (SMC) strategy is applied to maintain voltage stability, and its performance is compared with a traditional proportional-integral (PI) controller. Simulations in MATLAB/Simulink demonstrate that SMC offers better dynamic performance, including minimal overshoot, faster response, and an impressive hydrogen production rate of 0.98 L/min (98% efficiency). By providing more consistent voltage to the electrolyzer, SMC significantly boosts overall system performance. These findings underline the potential of advanced control strategies, supported by real-world data, to make renewable hydrogen production more reliable and efficient.

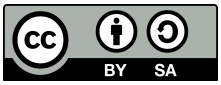

Corresponding Author:

Abdellah El Idrissi
Laboratory of Engineering Sciences and Energy Management (LASIME)
National School of Applied Sciences, Ibn Zohr University
Agadir 80000, Morocco
Email: abdellah.elidrissi@edu.uiz.ac.ma

1. INTRODUCTION

The accelerating depletion of fossil fuels, coupled with the urgent need to mitigate climate change, has intensified the global transition toward cleaner and more sustainable energy systems. Among the emerging solutions, green hydrogen that produced through electrolysis powered by renewable energy sources such as solar or wind, has gained prominence for its potential to decarbonize several sectors including industry, transportation, and power generation [1]. Morocco is well positioned to become a regional and global hub for green hydrogen production thanks to its abundant sunshine, renewable energy resources, and strategic proximity to major export markets. This potential is reinforced by the country's ambitious strategy, which includes large-scale investments in hydrogen and its derivatives, such as ammonia and methanol, thereby

consolidating its role in the global energy transition. In the broader context of carbon neutrality goals, green hydrogen emerges as an essential energy carrier, offering a path to decarbonization in hard-to-abate sectors while supporting the global transition to sustainable energy systems [2].

The electrolysis process involves splitting water molecules into hydrogen and oxygen using electricity from distributed energy sources (DES) like photovoltaic (PV) or wind system [3]. When powered by renewables, this process emits no carbon dioxide, making green hydrogen a truly clean energy carrier [4]. Current research focuses on improving electrolysis efficiency while optimizing the integration of DES with electrolyzer systems to ensure economic viability and operational stability [5]. Among the different types of electrolyzers, proton exchange membrane (PEM) electrolyzers stand out due to their fast response, compactness, and compatibility with variable inputs. However, coupling PEM systems with intermittent energy sources such as solar and wind remains technically challenging, primarily due to fluctuating voltage and current levels [6], [7]. Photovoltaic-powered PEM systems represent a promising configuration, but the variable nature of solar irradiance—affected by factors like cloud cover, time of day, and temperature—introduces issues that impact hydrogen production rates and electrolyzer durability [8], [9]. To address this, advanced control strategies are necessary to maintain voltage stability, reduce energy losses, and ensure continuous hydrogen generation under changing environmental conditions [10]. Given the PEM electrolyzer's requirement for low voltage and high current, integrating a DC-DC buck converter becomes essential to adapt the PV output to the required input levels [11], [12]. The performance of this power conditioning stage strongly depends on the effectiveness of its control method. Traditionally, proportional integral (PI) controllers have been employed in PV-electrolyzer systems due to their simplicity and satisfactory steady-state performance [13], [14]. However, they often fall short under dynamic and nonlinear operating conditions, which are common in solar-powered systems. to overcome this challenges, more advanced control strategies have been introduced such as fuzzy logic control (FLC) [15], [16], model predictive control (MPC) [17], and neural networks (NN) [18] have demonstrated better adaptability to system uncertainties and disturbances. Nevertheless, their implementation can be complex and computationally demanding, limiting their widespread deployment.

Out of the various robust control strategies, sliding mode control (SMC) has emerged as a particularly attractive option for PV–PEM hydrogen production systems due to its insensitivity to parameter variations, fast dynamic response, and strong disturbance rejection capabilities [19]. In dynamic solar environments, conventional controllers such as PI often suffer from slower transient response, sensitivity to parameter changes, and performance degradation under rapid irradiance and temperature fluctuations. In contrast, SMC offers superior robustness, faster convergence, and better tracking accuracy, making it highly effective for maintaining voltage stability and optimizing hydrogen production efficiency. Its ability to handle system nonlinearities, parameter variations, and external disturbances ensures stable operation and high efficiency, even under rapidly changing solar input. By effectively managing these dynamic conditions, SMC enhances both system reliability and hydrogen yield. Unlike previous studies that rely on idealized or simulated solar profiles, this work distinguishes itself by employing real-world solar data collected from an operational PV installation at the Higher School of Technology of Agadir. This enables a more accurate evaluation of control strategies under realistic environmental variations. The performance of SMC is compared with that of a conventional PI controller, with the goal of enhancing system stability, hydrogen production efficiency, and overall operational robustness under fluctuating solar conditions.

2. DESCRIPTION AND DESIGN OF THE SYSTEM

The photovoltaic hydrogen production system studied in this work is shown in Figure 1, It comprises a PV array, a DC-DC buck converter, and a PEM electrolyzer. The PV array converts solar irradiance into DC electricity, while a control unit regulates the voltage to match system requirements. The buck converter adjusts this voltage to the level needed by the electrolyzer, which then uses the regulated power to perform water electrolysis for hydrogen production and storage.

2.1. Model of the PEM electrolyser

Modeling a proton exchange membrane (PEM) electrolyzer as an equivalent electrical circuit enables safe testing of control strategies without physical equipment. The model includes the reversible voltage E_{rev} and three resistances: R_{ohm} (internal losses), R_{act} (activation losses), and R_{con} (concentration limitations). The total voltage V_{elz} is given by (1) [20]. To analyze voltage and power variations with current, a commercial

400 W PEM electrolyzer was selected; its specifications are in Table 1. The system can be approximated linearly by a voltage source in series with resistance, described by (2).

$$V_{\text{elz}} = E_{\text{rev}} + I_{\text{elz}} \left(R_{\text{act}} + R_{\text{ohm}} + R_{\text{con}}\right) \quad (1)$$

$$V_{\text{elz}} = 0.0625 I_{\text{elz}} + 4.375 \quad (2)$$

The linear model coefficients were obtained by interpolating experimental data over a current range of 3–50 A [21], showing a nearly linear voltage–current relationship, as shown in Figure 2. This validates the simplified equivalent circuit model with a reversible voltage source and a resistive component. Hydrogen production ($\dot{N}_{H_2}$) is calculated using Faraday's law [22].

$$\dot{N}_{H_2} = \frac{nI}{2F} \quad \text{(moles/s)}, \quad \dot{N}_{H_2} = 0.00696\, nI \quad \text{(L/min)} \quad (3)$$

Where n is the number of cells, I the applied current, and F Faraday's constant. Faraday efficiency (η_F) expresses the fraction of charge converted into hydrogen, as in (4).

$$\eta_F = \frac{\text{Actual moles of } H_2}{\text{Theoretical moles of } H_2} \times 100\% \quad (4)$$

Higher efficiency increases hydrogen yield and reduces energy consumption.

2.2. Solar PV array

The solar PV unit is used to produce power output. The solar panel in this article is a single unit with a maximum power input capacity of 120.7 W. The solar module specifications are shown in Table 2 [23].

Table 1. PEM electrolyzer specifications

Specification	Values (unit)
Rated power (P_{el})	400 W
Operating voltage (V_{elz})	2.2–8 V
Electrolyzer current (I_{elz})	0–50 A
Output pressure	0.1–10.5 bar
H_2 flow rate	1 L/min
(T = 20 °C, P = 1 bar)	
Cell Numbers	3

Table 2. Solar panel parameters for Waaree Energies WU-120

Parameters	Value
I_{mp}	7.1 A
V_{mp}	17 V
$P_{\text{max,e}}$	120.7 W
I_{sc}	8 A
V_{oc}	21 V
PV solar irradiation (G)	1000 W/m²
PV operation temperature (T)	25 °C

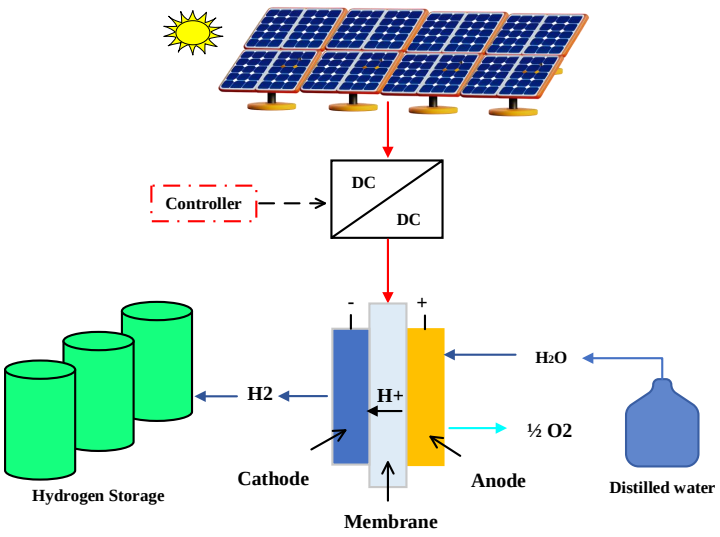

Figure 1. Schematic of the proposed system to produce hydrogen using solar energy

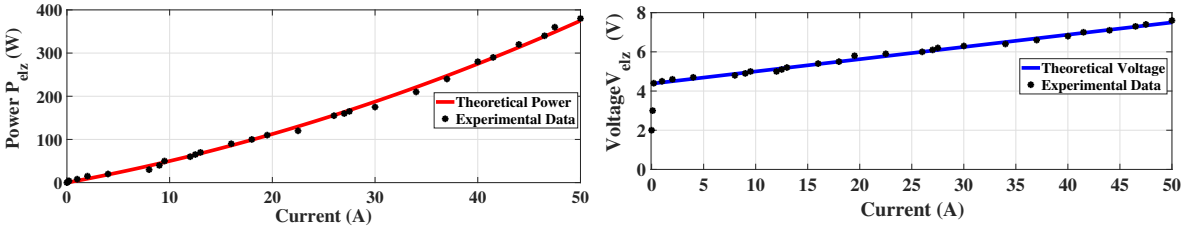

(a) (b)

Figure 2. Static characteristics of the selected PEM electrolyzer cells: (a) electrolyzer power vs. current and (b) voltage vs. current, with experimental data (o) and model fitting (solid line)

2.3. Modeling of buck converter

The buck converter is a type of DC-DC converter that is widely used in power electronics applications due to its simplicity, efficiency, and ability to step down the input voltage. The converter consists of a switch (S), an inductor (L), a diode (D), and a capacitor (C). Electrolyzers typically operate at a low DC voltage for water electrolysis, so the use of a DC-DC converter, as shown in Figure 3 is essential. In addition to reducing the voltage, these converters manage voltage adaptation to handle fluctuations in the voltage provided by the solar panels. By selecting the appropriate components and adjusting the converter parameters according to the specific application requirements, we minimize power losses, and extend the life of the components [24]. Table 3 shows the sizing of the various components of the buck converter.

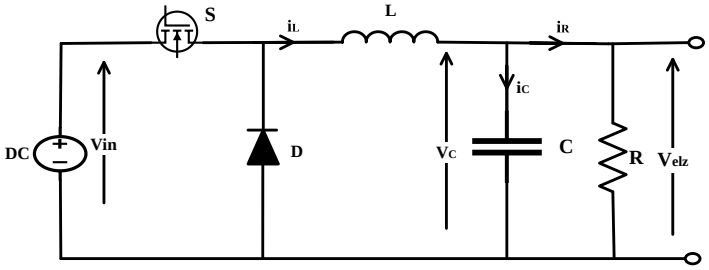

Figure 3. Electrical schematic of the DC-DC buck converter

Table 3. Buck converter parameters

Parameters	Values
Inductor L	497 µH
Capacitor C	7.94 µF
Switching frequency f	40 kHz
Duty cycle α	22.8%
Input voltage V_{in}	30 V
Output voltage v_{elz}	7.5 V

The buck converter operates in two modes depending on the switch state. When ON, the inductor and capacitor dynamics are governed by (5).

$$\frac{di_L}{dt} = \frac{V_{\text{in}} - v_{\text{elz}}}{L}, \quad \frac{dv_{\text{elz}}}{dt} = \frac{i_L}{C} - \frac{v_{\text{elz}}}{RC} \tag{5}$$

When OFF as in (6).

$$\frac{di_L}{dt} = -\frac{v_{\text{elz}}}{L}, \quad \frac{dv_{\text{elz}}}{dt} = \frac{i_L}{C} - \frac{v_{\text{elz}}}{RC} \tag{6}$$

These can be written in the state-space form as (7).

$$\dot{x} = Ax + BV_{\text{in}}, \quad Y = Nx \tag{7}$$

Where:

$$x = \begin{bmatrix} i_L \\ v_{\text{elz}} \end{bmatrix}, \quad N = \begin{bmatrix} 0 & 1 \end{bmatrix}$$

State-space averaging over one switching period, as (8).

$$A = \alpha A_1 + (1-\alpha)A_2, \quad B = \alpha B_1 \tag{8}$$

With:

$$A_1 = A_2 = \begin{bmatrix} -\frac{1}{L} & 0 \\ \frac{1}{C} & -\frac{1}{RC} \end{bmatrix}, \quad B_1 = \begin{bmatrix} \frac{1}{L} \\ 0 \end{bmatrix}$$

The averaged model becomes (9).

$$\dot{x} = \begin{bmatrix} -\frac{(1-\alpha)}{L} & 0 \\ \frac{(1-\alpha)}{C} & -\frac{1}{RC} \end{bmatrix} x + \begin{bmatrix} \frac{1}{L} \\ 0 \end{bmatrix} V_{\text{in}} \tag{9}$$

3. CONTROL STRATEGIES

Sliding mode controller (SMC) is a powerful control technique that can provide fast and robust control of systems. Its effectiveness has been demonstrated in various applications, including DC-DC converters, where it can provide superior performance compared to other control techniques [25]. The control variable x_{Buck} is presented in (10), where the variables x_1, x_2, and x_3 are respectively the voltage error, the derivative of the error, and the integral of the error. The instantaneous capacitor, inductor, and load currents, respectively; V_{ref}, v_i, and βv_{elz} denote the reference, instantaneous input, and instantaneous output voltages, respectively; β denotes the feedback network ratio; and $u = 0$ or 1 is the switching state of power switch SW. The equation of state for the control system in the vector space is written in (10).

$$x_{\text{Buck}} = \begin{cases} x_1 = V_{\text{ref}} - \beta v_{\text{elz}} \\ x_2 = \dot{x}_1 = \frac{d}{dt}(V_{\text{ref}} - \beta v_{\text{elz}}) \\ x_3 = \int x_1 \, dt = \int (V_{\text{ref}} - \beta v_{\text{elz}}) \, dt \end{cases} \quad \text{and} \quad \dot{x}_{\text{Buck}} = \begin{cases} \dot{x}_1 = x_2 \\ \dot{x}_2 = -\frac{1}{RC} x_2 + \frac{\beta v_{\text{in}}}{LC} u + \frac{\beta v_{\text{elz}}}{LC} \\ \dot{x}_3 = x_1 \end{cases} \tag{10}$$

The state-space model describing the system can be derived as (11).

$$\dot{x}_{\text{Buck}} = \begin{bmatrix} 0 & 1 & 0 \\ 0 & -\frac{1}{RC} & 0 \\ 1 & 0 & 0 \end{bmatrix} x + \begin{bmatrix} 0 \\ -\frac{\beta v_{\text{in}}}{LC} \\ 0 \end{bmatrix} u_{\text{eq}} + \begin{bmatrix} 0 \\ \frac{\beta v_{\text{elz}}}{LC} \\ 0 \end{bmatrix} \tag{11}$$

The SMC law uses a switching function to determine the control signal, as (12).

$$u = \begin{cases} 1 & \text{when } S > 0 \\ 0 & \text{when } S < 0 \end{cases} \quad \text{where } S \text{ defined as} \quad S = a_1 x_1 + a_2 x_2 + a_3 x_3 = J^T x \tag{12}$$

Where S is the instantaneous state trajectory and $J^T = [a_1, a_2, a_3]$ and a_1, a_2, a_3 are the sliding coefficients. The sliding mode control ensures that the system meets the sliding conditions: hitting, existence, and stability.

The ramp signal and control signal are compared to get the output switching signal, which has a frequency identical to the ramp signal. By fixing the ramp signal frequency, the output switching signal frequency remains constant. Therefore, using the PWM technique in controller design ensures a fixed frequency for the proposed method. In the first step, the equivalent control signal u_{eq} is derived using the invariance condition. In the second step, u_{eq} is translated to the duty ratio α of the PWM during the derivation process. The equivalent control signal u_{eq} is obtained from the equation $\dot{S} = J^T Ax + J^T B u_{eq} + D = 0$, which yields the equivalent control function, as (13). Solving for u_{eq}:

$$u_{eq} = -\frac{\beta L}{\beta v_{in}} \left(\frac{a_1}{a_2} - \frac{1}{RC} \right) i_C + \frac{a_3 LC}{a_2 \beta v_{in}} \left(V_{ref} - \beta v_{elz} \right) + \frac{v_{elz}}{v_{in}} \tag{13}$$

Translating the equivalent control as in (13) to the duty ratio α, where $0 < \alpha = \frac{v_c}{\hat{v}_{\text{ramp}}} < 1$, gives the following relationships for the control signal v_c and ramp signal $\hat{v}_{\text{ramp}}$ as in (14). For the practical implementation of the PWM-based sliding mode controller, the electrical schematic of the SMC controller is shown in Figure 4.

$$v_c = u_{\text{eq}} = k_1 i_C + k_2(V_{\text{ref}} - \beta v_{\text{elz}}) + \beta v_{\text{elz}} \quad \text{and} \quad \hat{v}_{\text{ramp}} = \beta v_{\text{in}} \tag{14}$$

Where:

$$k_1 = -\beta L \left(\frac{a_1}{a_2} - \frac{1}{RC} \right), \quad k_2 = \frac{a_3}{a_2} LC$$

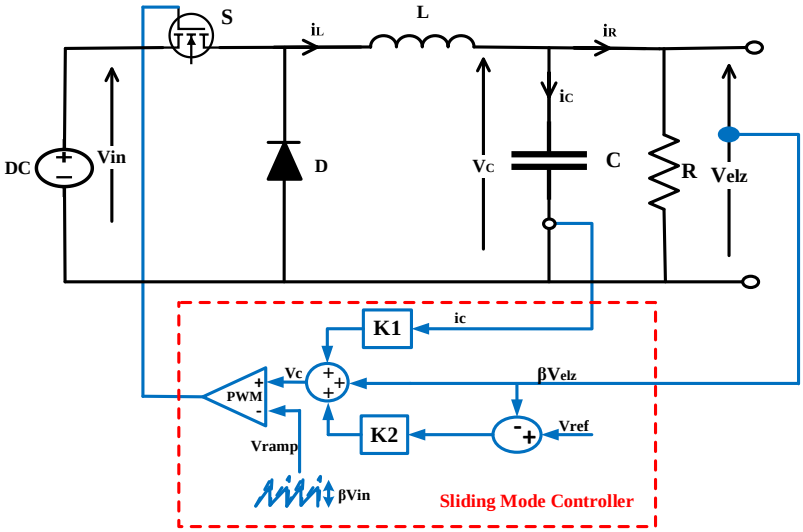

Figure 4. Electrical schema of SMC controller

4. RESULTS AND DISCUSSION

4.1. Steady-state performance

To verify the efficacy of sliding mode control in regulating voltage to the desired value for powering the electrolyzer used in the study, we compare the results obtained using this method with those obtained using a classical PI controller, which was also employed for the same purpose. We used the MATLAB/Simulink platform for this comparison. The steady-state operational conditions of the system, including the solar PV parameters, buck converter, and PEM electrolyzer, are shown under rated conditions. The solar iradiation is fixed at 1000 W/m², and the temperature is held at 25 °C. The solar panel voltage, current, and power are stable at 30 V, 30 A, and 897 W, respectively, under full irradiance. These values indicate that the PV system is operating at its full rated capacity. The PEM electrolyzer, powered by the solar PV, also operates at full rated power under these conditions. The steady-state electrolyzer voltage (7.5 V), current (47.15 A), and power (354 W) are achieved by both PI and SMC control strategies, Figure 5 illustrates the performance of both control methods. In Figure 5(a), we observe the electrolyzer voltage (V_{elz}), and in Figure 5(b), the hydrogen production rate (H_2). Both controllers successfully ensure stable operation, with the voltage settling around 7.5 V and the hydrogen production rate stabilizing at approximately 0.985 L/min. These results confirm the system's effective and reliable performance under steady-state conditions.

However, as demonstrated in Figure 5, the SMC proves to be slightly more accurate and precise than the PI controller in steady-state mode. The results show that the SMC performs significantly better than the PI controller in terms of stability, accuracy, and response time. In summary, the SMC's lower values across both system response and error metrics make it the more effective controller, with greater stability, faster settling, and a much lower error profile compared to the PI controller.

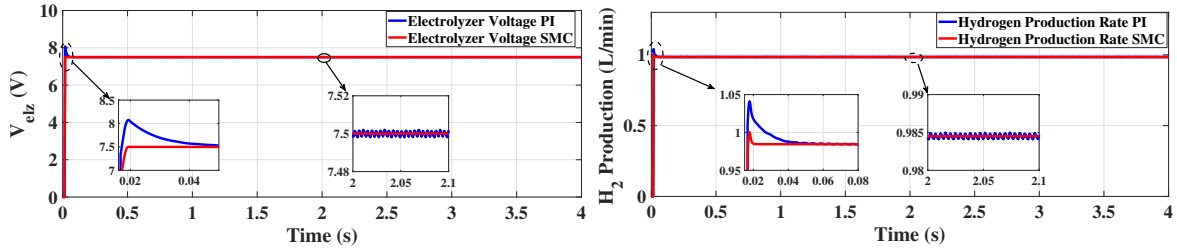

(a) (b)

Figure 5. Performance of the system under constant solar irradiation: (a) the electrolyzer voltage (V_{elz}) and (b) the hydrogen production rate (H_2)

4.2. Dynamic performance

In order to evaluate the dynamic performance of our controller, we used experimental data collected from a photovoltaic panel installed on the rooftop of our laboratory at the Higher School of Technology of Agadir. The dataset includes solar irradiance, panel surface temperature, and output voltage. illustrated in Figure 6, the data show noticeable fluctuations: irradiance ranges from 400 W/m^2 to 1000 W/m^2, while the surface temperature of the PV panel varies between 42 °C and 62 °C, as shown in Figures 6(a) and 6(b). These variations directly affect key PV system parameters, particularly the panel voltage (V_{pv}), depicted in Figure 6(c), and panel power (P_{pv}) in Figure 6(d) respectively. The irradiance profile initially shows a steady increase, followed by a sharp decline near the midpoint, indicating a temporary drop in solar input. This change is clearly reflected in the corresponding voltage and current responses of the system.

The results in Figures 7(a) and 7(b) reveal that the SMC consistently outperforms the PI controller in terms of stability, accuracy, and dynamic response. The SMC demonstrates minimal overshoot at 0.0299%, significantly lower than the PI's 12.2873%, indicating a more controlled and steady response close to the target value. While both controllers exhibit rapid response times, the SMC achieves a much faster settling time of 0.0032 seconds compared to the PI's 0.0267 seconds. Additionally, the SMC has a lower mean absolute percentage error (MAPE) of 0.21%, is significantly lower for the SMC, indicating better accuracy in achieving the desired output. Here, V_{ref} represents the desired value (7.5 V) $y_{\text{actual},i}$ is the actual response at each time step i, and n is the number of time steps. contrasting sharply with the PI's 6.96%, further emphasizing its superior tracking accuracy, When examining error metrics, the SMC again distinguishes itself with superior performance indices. The error signal is defined as $e(t) = V_{\text{ref}} - V_{\text{elz}}(t)$.

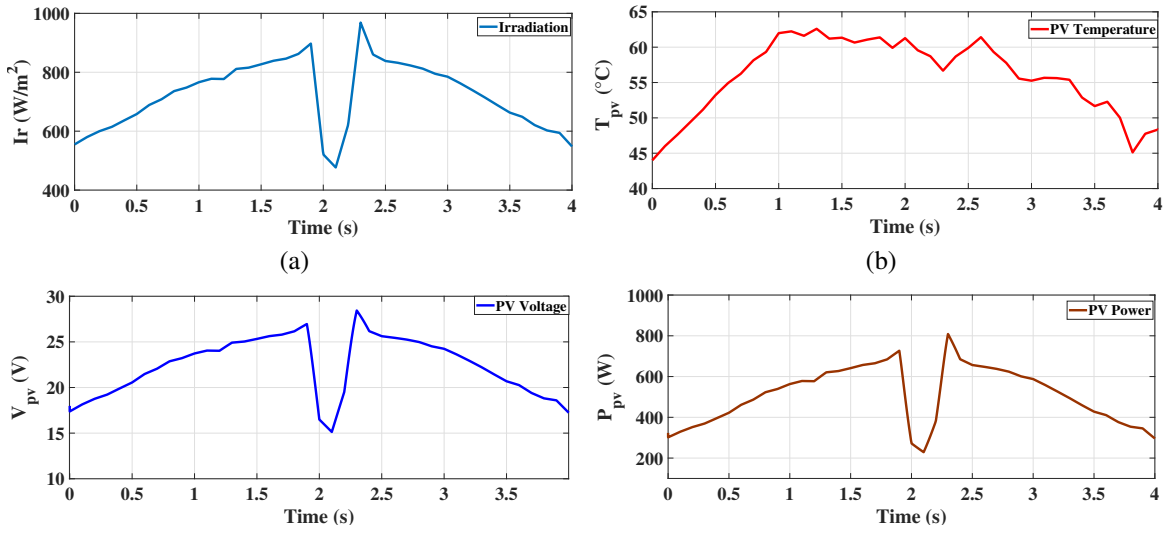

(a) (b) (c) (d)

Figure 6. Dynamic performance of the system: (a) solar irradiance (I_r), (b) temperature of the photovoltaic panel (T_{pv}), (c) the panel voltage (V_{pv}), and (d) the panel power (P_{pv})

Where V_{ref} (7.5 V) is the desired voltage and $V_{\text{elz}}(t)$ is the actual electrolyzer voltage at time t, the integral of squared error (ISE) for the SMC is lower at 0.0386 compared to 0.0476 for the PI controller, reflecting a more efficient reduction in overall error energy. Similarly, the integral of absolute error (IAE) is significantly reduced to 0.0114 for the SMC, whereas the PI controller reaches 0.1362. The most notable improvement appears in the integral of time-weighted absolute error (ITAE), where the SMC achieves a remarkably low value of 0.0039, in contrast to 0.2378 for the PI controller. These results confirm that the SMC not only minimizes the overall error but also reacts more promptly to disturbances, resulting in smoother and more accurate system performance, Table 4 summarizes the dynamic performance and error metrics of both controllers.

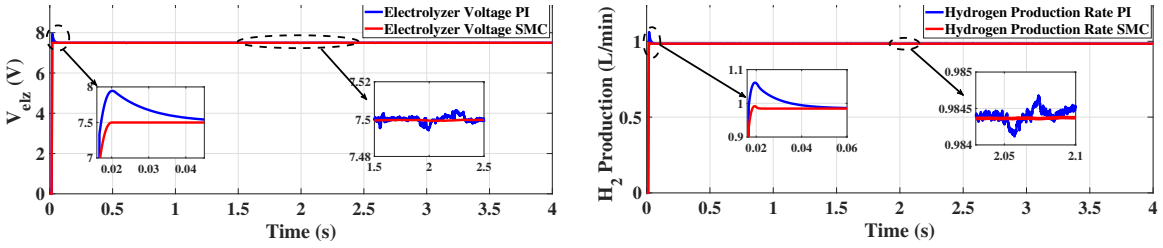

(a) (b)

Figure 7. Dynamic performance of the system with varying solar irradiation and temperature: (a) the electrolyzer voltage (V_{elz}) and (b) the hydrogen production rate (H_2)

Table 4. Dynamic performance and error metrics of controllers

Controller	MAPE (%)	Settling time (s)	Overshoot (%)	ISE	IAE	ITAE
Equation	–	–	–	$\int e^2(t)\,dt$	$\int \lvert e(t)\rvert\,dt$	$\int t\lvert e(t)\rvert\,dt$
PI	6.96	0.0267	12.2873	0.0476	0.1362	0.2378
SMC	0.21	0.0032	0.0299	0.0386	0.0114	0.0039

5. CONCLUSION

This study investigated the use of advanced control techniques, particularly sliding mode control (SMC), to address the challenges of integrating fluctuating renewable energy sources with PEM electrolyzers for green hydrogen production. The system includes a photovoltaic array connected to an electrolysis unit via a DC-DC buck converter, which adjusts the solar panel voltage to the level needed by the electrolyzer. MATLAB/Simulink simulations demonstrated that SMC outperforms the traditional PI controller by achieving nearly zero overshoot, a very fast settling time of 0.003 seconds, and a low error rate (MAPE of 0.21%). Additionally, SMC enabled a high hydrogen production rate of 0.98 liters per minute with 98% efficiency, thanks to its ability to provide a stable and consistent voltage to the electrolyzer. These results underscore the potential of advanced control strategies, supported by real-world data, to enhance the reliability and efficiency of renewable hydrogen production, laying a solid foundation for future work aimed at further optimizing control methods and improving system performance.

FUNDING INFORMATION

Authors state no funding involved.

AUTHOR CONTRIBUTIONS STATEMENT

This journal uses the Contributor Roles Taxonomy (CRediT) to recognize individual author contributions, reduce authorship disputes, and facilitate collaboration.

Name of Author	C	M	So	Va	Fo	I	R	D	O	E	Vi	Su	P	Fu
Abdellah El Idrissi	✓	✓	✓	✓	✓	✓	✓	✓	✓	✓	✓		✓	
Belkasem Imodane	✓	✓	✓	✓	✓		✓		✓	✓	✓			
M'hand Oubella	✓	✓	✓	✓	✓	✓	✓		✓		✓	✓	✓	
Hatim Ameziane	✓	✓		✓	✓		✓	✓	✓	✓	✓			
Mohamed Benydir	✓	✓	✓	✓	✓				✓	✓	✓			
Kaoutar Dahmane		✓	✓	✓	✓	✓		✓		✓	✓			
Driss Belkhiri		✓		✓	✓					✓	✓			
Mohamed Ajaamoum	✓	✓	✓	✓	✓	✓	✓		✓		✓	✓	✓	

C : **C**onceptualization
M : **M**ethodology
So : **So**ftware
Va : **Va**lidation
Fo : **Fo**rmal Analysis
I : **I**nvestigation
R : **R**esources
D : **D**ata Curation
O : Writing - **O**riginal Draft
E : Writing - Review & **E**diting
Vi : **Vi**sualization
Su : **Su**pervision
P : **P**roject Administration
Fu : **Fu**nding Acquisition

CONFLICT OF INTEREST STATEMENT

The authors declare that they have no known competing financial interests or personal relationships that could have appeared to influence the work reported in this paper.

DATA AVAILABILITY

The MATLAB simulation data that support the findings of this study will be made available in an open-access repository upon acceptance of the manuscript.

REFERENCES

[1] T.-Z. Ang, M. Salem, M. Kamarol, H. S. Das, M. A. Nazari, and N. Prabaharan, "A comprehensive study of renewable energy sources: classifications, challenges and suggestions," *Energy Strategy Reviews*, vol. 43, p. 100939, Sep. 2022, doi: 10.1016/j.esr.2022.100939.

[2] A. Caillard, R. Yeganyan, C. Cannone, F. Plazas-Niño, and M. Howells, "A critical analysis of Morocco's green hydrogen roadmap: a modelling approach to assess country readiness from the energy trilemma perspective," *Climate*, vol. 12, no. 5, p. 61, Apr. 2024, doi: 10.3390/cli12050061.

[3] P. Fernández-Arias, Á. Antón-Sancho, G. Lampropoulos, and D. Vergara, "On green hydrogen generation technologies: a bibliometric review," *Applied Sciences*, vol. 14, no. 6, p. 2524, Mar. 2024, doi: 10.3390/app14062524.

[4] W. Mei, L. Sun, and Y. Zhao, "Overview of hydrogen energy and general aspects of water electrolysis," in *Green Hydrogen Production by Water Electrolysis*, Boca Raton: CRC Press, 2024, pp. 1–26, doi: 10.1201/9781003368939-1.

[5] M. Koundi *et al.*, "Investigation of hydrogen production system-based PEM EL: PEM EL modeling, DC/DC power converter, and controller design approaches," *Clean Technologies*, vol. 5, no. 2, pp. 531–568, Apr. 2023, doi: 10.3390/cleantechnol5020028.

[6] A. Baraean, M. Kassas, M. S. Alam, and M. A. Abido, "Physics-informed NN-based adaptive backstepping terminal sliding mode control of buck converter for PEM electrolyzer," *Heliyon*, vol. 10, no. 7, p. e29254, Apr. 2024, doi: 10.1016/j.heliyon.2024.e29254.

[7] S. G. Nnabuife, A. K. Hamzat, J. Whidborne, B. Kuang, and K. W. Jenkins, "Integration of renewable energy sources in tandem with electrolysis: A technology review for green hydrogen production," *International Journal of Hydrogen Energy*, vol. 107, pp. 218–240, Mar. 2025, doi: 10.1016/j.ijhydene.2024.06.342.

[8] I. Arias *et al.*, "Assessing system-level synergies between photovoltaic and proton exchange membrane electrolyzers for solar-powered hydrogen production," *Applied Energy*, vol. 368, p. 123495, Aug. 2024, doi: 10.1016/j.apenergy.2024.123495.

[9] H. A. Z. AL-bonsrulah *et al.*, "Design and simulation studies of hybrid power systems based on photovoltaic, wind, electrolyzer, and PEM fuel cells," *Energies*, vol. 14, no. 9, p. 2643, May 2021, doi: 10.3390/en14092643.

[10] D. Y. Gavrailov, S. V. Boycheva, and X. Gao, "A direct coupled photovoltaic - electrolyser system for producing green hydrogen," *IOP Conference Series: Earth and Environmental Science*, vol. 1380, no. 1, 2024, doi: 10.1088/1755-1315/1380/1/012010.

[11] A. Alobaid and R. A. Adomaitis, "Optimal design of a coupled photovoltaic–electrolysis-battery system for hydrogen generation," *Sustainable Energy & Fuels*, vol. 7, no. 6, pp. 1395–1414, 2023, doi: 10.1039/D2SE01555B.

[12] M. Chen, S.-F. Chou, F. Blaabjerg, and P. Davari, "Overview of power electronic converter topologies enabling large-scale hydrogen production via water electrolysis," *Applied Sciences*, vol. 12, no. 4, p. 1906, Feb. 2022, doi: 10.3390/app12041906.

[13] M. E. Şahin, "A photovoltaic powered electrolysis converter system with maximum power point tracking control," *International Journal of Hydrogen Energy*, vol. 45, no. 16, pp. 9293–9304, Mar. 2020, doi: 10.1016/j.ijhydene.2020.01.162.

[14] R. K. Kumar and P. Samuel, "Designing a hydrogen generation system through PEM water electrolysis with the capability to adjust fast fluctuations in photovoltaic power," *International Journal of Hydrogen Energy*, vol. 82, pp. 1–10, Sep. 2024, doi: 10.1016/j.ijhydene.2024.07.376.

[15] M. Benydir, M. Oubella, S. Mouslim, M. Ajaamoum, K. Dahmane, and B. Imoudane, "Implementation and analysis of a fuzzy logic and sliding mode controller on a boost DC/DC converter in a PV array," *International Journal of Renewable Energy Research*, vol. 12, no. 1, pp. 294–301, 2023, doi: 10.20508/ijrer.v13i1.13862.g8683.
[16] B. Imodane, M. Benydir, B. Bouachrine, M. Ajaamoum, and K. Dahmane, "Experimental validation of two voltage regulation strategies for boost converters in wind systems," *International Journal of Power Electronics and Drive Systems (IJPEDS)*, vol. 16, no. 1, pp. 509–518, Mar. 2025, doi: 10.11591/ijpeds.v16.i1.pp509-518.
[17] W. El Aouni and L. A. Dessaint, "Real-time implementation of input-state linearization and model predictive control for robust voltage regulation of a DC-DC boost converter," *IEEE Access*, vol. 8, pp. 192101–192108, 2020, doi: 10.1109/ACCESS.2020.3032327.
[18] S. D. Gangula, T. K. Nizami, R. R. Udumula, A. Chakravarty, and P. Singh, "Adaptive neural network control of DC–DC power converter," *Expert Systems with Applications*, vol. 229, p. 120362, Nov. 2023, doi: 10.1016/j.eswa.2023.120362.
[19] Y. Mousavi, G. Bevan, I. B. Kucukdemiral, and A. Fekih, "Sliding mode control of wind energy conversion systems: trends and applications," *Renewable and Sustainable Energy Reviews*, vol. 167, 2022, doi: 10.1016/j.rser.2022.112734.
[20] D. S. Falcão and A. M. F. R. Pinto, "A review on PEM electrolyzer modelling: guidelines for beginners," *Journal of Cleaner Production*, vol. 261, p. 121184, Jul. 2020, doi: 10.1016/j.jclepro.2020.121184.
[21] F. Alonge, S. M. Collura, F. D'Ippolito, D. Guilbert, M. Luna, and G. Vitale, "Design of a robust controller for DC/DC converter–electrolyzer systems supplied by μWECSs subject to highly fluctuating wind speed," *Control Engineering Practice*, vol. 98, p. 104383, May 2020, doi: 10.1016/j.conengprac.2020.104383.
[22] B. Yodwong, D. Guilbert, M. Phattanasak, W. Kaewmanee, M. Hinaje, and G. Vitale, "Faraday's efficiency modeling of a proton exchange membrane electrolyzer based on experimental data," *Energies*, vol. 13, no. 18, p. 4792, Sep. 2020, doi: 10.3390/en13184792.
[23] L. Nadam, M. Chakravarthy, and M. Manjula, "Optimized energy management for PV hybrid power systems with DC bus voltage control," *International Journal of Electrical and Electronics Research*, vol. 12, no. 4, pp. 1173–1180, 2024, doi: 10.37391/IJEER.120407.
[24] N. Deshmukh, S. Prabhakar, and S. Anand, "Power loss reduction in buck converter based active power decoupling circuit," *IEEE Transactions on Power Electronics*, vol. 36, no. 4, pp. 4316–4325, 2020, doi: 10.1109/TPEL.2020.3024721.
[25] Ö. Türksoy and A. Türksoy, "A fast and robust sliding mode controller for automatic voltage regulators in electrical power systems," *Engineering Science and Technology*, an International Journal, vol. 53, 2024, doi: 10.1016/j.jestch.2024.101697.

BIOGRAPHIES OF AUTHORS

Abdellah El Idrissi is an Ph.D. student in engineering sciences at Ibn Zohr University (UIZ), Agadir, Morocco, and a member of Laboratory of Engineering Sciences and Energy Management (LASIME) at the High School of Technologies of Agadir (ESTA). His doctoral research focuses on renewable energy systems for hydrogen production, emphasizing the optimization of solar-powered electrolyzers through advanced control strategies and the integration of power electronics. He can be contacted at email: abdellah.elidrissi@edu.uiz.ac.ma.

Belkasem Imodane is an Ph.D. student in electrical engineering at the University of Ibn Zohr, Agadir. He graduated as an embedded systems engineer in 2021 from the National School of Applied Sciences, Agadir, Morocco. Subsequently, he joined the research group at the Engineering Sciences and Energy Management Laboratory, University of Ibn Zohr, Agadir, Morocco. His research focuses on renewable energies for his doctoral thesis. He can be contacted at email: b.imodane@uiz.ac.ma.

M'hand Oubella holds the position of professor in higher education at the High School of Technologies of Agadir (ESTA), Ibn Zohr University, Agadir, Morocco. He obtained his Ph.D. in energetic and process engineering from the National School of Applied Sciences (ENSA) of Agadir in 2014. Currently, M'hand Oubella is a member of the Laboratory of Engineering Sciences and Energy Management (LASIME) at the High School of Technologies of Agadir (ESTA), and his research focuses on intelligent systems and energy management, with a particular emphasis on renewable energies. This research is conducted within the framework of the research team known as Intelligent Systems and Energy Management (ERSIME). He can be contacted at email: m.oubella@uiz.ac.ma.

Hatim Ameziane received his M.S. and Ph.D. in electrical engineering from the Sidi Mohamed Ben Abdellah University in 2014 and 2020, respectively. He is currently an assistant professor in the Electrical Engineering Department at the National School of Applied Sciences (ENSA– Sultan Moulay Slimane University) and a principal research scientist at the Science and Technology for the Engineer Laboratory (LaSTI), where he focuses on research in renewable energy, machine learning, power management ICs design, and CMOS mixed-signal integrated circuits for embedded systems. He can be contacted at email: h.ameziane@usms.ma.

Mohamed Benydir is a specialist in electrical engineering, automation, and renewable energies, he holds a Ph.D. in electrical engineering, automation, and renewable energies from the National School of Applied Sciences (ENSA) in Agadir. Originally from Agadir, Morocco, his research focuses on renewable energy, engineering science, and energy management. He can be contacted at email: mohamed.benydir@edu.uiz.ac.ma.

Kaoutar Dahmane is a Ph.D. student in engineering sciences at the Ibn Zohr University (UIZ) of Agadir. She is originally from Ouarzazate, Morocco. As a researcher student, she addresses key questions in relation to power system and renewable energy. The main aim of her doctoral thesis is to perform power quantity and quality controls in grid-connected renewable energy systems. She can be contacted at email: kaoutar.dahmane@edu.uiz.ac.ma.

Driss Belkhiri holds a Ph.D. in electrical engineering and renewable energy from the Ibn Zohr University, Agadir, Morocco. His research focuses on renewable energy technologies, including wind energy systems, green hydrogen, and control and automation systems, with a particular emphasis on artificial intelligence techniques such as artificial neural networks and fuzzy logic. His doctoral work was conducted within the research team of the Laboratory of Engineering Sciences and Energy Management (LASIME) in Agadir, Morocco. He can be contacted at email: driss.belkhiri@edu.uiz.ac.ma.

Mohamed Ajaamoum is an professor Ph.D. at the Department of Electrical Engineering, High School of Technology of Agadir, Ibn Zohr University, Agadir, Morocco. His research interests are in photovoltaic systems, fuzzy control, neural network, renewable energy technologies, system modeling, and power electronics. He can be contacted at email: m.ajaamoum@uiz.ac.ma.